Hindawi
Mathematical Problems in Engineering
Volume 2018, Article ID 4394058, 20 pages
https://doi.org/10.1155/2018/4394058

Research Article

Dynamical Behaviors of Coupled Memristor-Based Oscillators with Identical and Different Nonlinearities

A. Elsonbaty, A. Abdelkhalek, and A. Elsaid

Mathematics and Engineering Physics Department, Faculty of Engineering, Mansoura University, Egypt

Correspondence should be addressed to A. Elsonbaty; amrelsonbaty@mans.edu.eg

Received 28 May 2018; Accepted 2 September 2018; Published 21 October 2018

Academic Editor: Alessandro Lo Schiavo

In this work, the interesting dynamics of coupled nonlinear memristor-based oscillators in ring configuration are explored. The mathematical models are derived to describe the possible cases of employing identical or different nonlinearities. Analytical and numerical techniques, involving perturbation methods, normal forms, phase portraits, and Lyapunov exponents are used to investigate various types of dynamical behaviors along with their stability regions in parameters space. The effects of time-delayed coupling on the proposed system are numerically studied. It is demonstrated that the coupled oscillators show rich dynamics including periodic orbits, quasiperiodicity, two-dimensional, and three-dimensional tori.

1. Introduction

Many applications in engineering, physics, chemistry, biology, and economy are modeled using nonlinear differential equations (DEs) where their exact forms of solutions are very difficult to obtain in general or they do not provide tools to understand the underlying dynamics. However, dynamical systems methods provide powerful techniques to study the qualitative behaviors of mathematical model solution rather than quantitative ones [1].

One of the interesting problems in nonlinear theory is to study the dynamics of systems involving coupled nonlinear oscillators. This problem appears in many applications in biology [2], neuroscience [3–6], chemistry [7, 8], and physics [9–11]. Researchers in the field of dynamical systems are interested in studying the stability of coupled oscillators systems with nonlinear properties since 1950s till now [12–15].

In 1970, Chua introduced the fourth electronic element called the memristor [16]. It is a two-terminal element that relates the magnetic flux ϕ between the terminals with the electric charge q that passes through it [16, 17]. Studies on the dynamical properties, i.e., stability and bifurcation of the memristor-based oscillator circuit, have received increasing interest [18–21]. The main reason is that coupled memristor-based oscillatory circuits appear in many applications such as filtering, energy storage, energy transmission, isolation impedance transformation, learning networks that require a synapse-like function, secure communications, and image stabilization [22–31].

In [32], the stability of three nonlinear identical memristor-based oscillators coupled by inductors in ladder circuit configuration was studied. In this paper, we examine a more generalized case by considering coupled three memristor-based oscillators in ring configuration where nonidentical memristors are allowed. Two cases are studied where both identical and different nonlinearities are considered. The memristor used is of a flux-controlled type that has memductance function $w(\phi)$ representing the flux-dependent rate of change of charge

$$w(\phi) = \frac{\mathrm{dq}(\phi)}{\mathrm{d}\phi}. \tag{1}$$

The two cases studied are according to the definition of $q(\phi)$. In the first case the memristors are described by three third-order polynomials, whereas in the second case one memristor is described by third-order polynomial while the remaining memristors are characterized by fourth-order polynomials.

Time delays play an important role in mathematical modeling of real systems and studying synchronization such that their effects cannot be neglected in real life; see, for

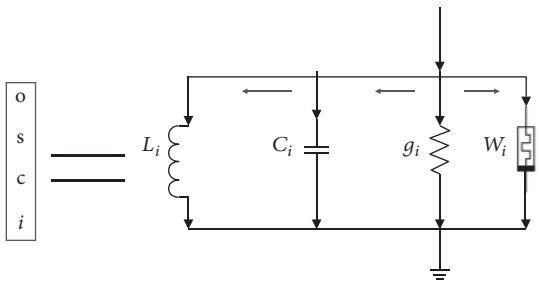

Figure 1: The ith memristor-based oscillator circuit in coupled network.

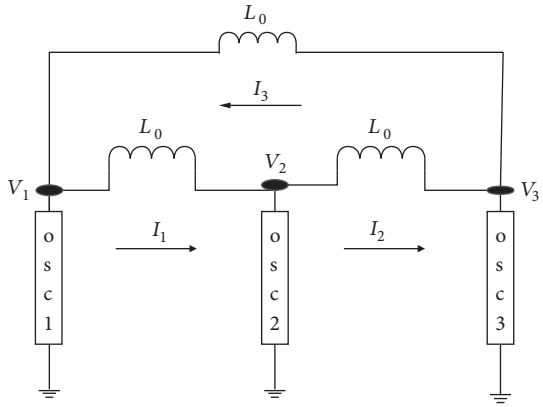

Figure 2: Ring type schematic of three coupled memristor-based oscillators where each oscillator is referred to as osc i, $i = 1, 2, 3$.

example, [33–35]. Therefore, numerical investigations of time-delayed coupling influences on coupled oscillators dynamics are carried out in this work. The rest of the paper is organized as follows: In Section 2, mathematical models of all cases studied in this work are presented. In Section 3, the multiple scales method is applied to acquire the normal form for each system. In Section 4, various types of dynamical behaviors that can be extracted from normal forms in addition to their stability analysis are obtained. In Section 5, numerical simulations are carried out to verify theoretical results. The general discussion and main conclusion of this work are presented in Section 6.

2. Ring Model Equations

In this section, we derive the fundamental equations describing the three ring coupled oscillators circuit. Figure 1 shows the memristor-based oscillator circuit we adopt in this work. Applying Kirchhoff's voltage law (KVL) and Kirchhoff's current law (KCL) to the circuit in Figure 2, the model can be described as follows:

$$
\begin{aligned}
I_1 - I_3 + C_1\dot{V}_1 + g_1V_1 + I_{L_1} + I_{w_1}(V_1) &= 0,\\
I_2 - I_1 + C_2\dot{V}_2 + g_2V_2 + I_{L_2} + I_{w_2}(V_2) &= 0,\\
I_3 - I_2 + C_3\dot{V}_3 + g_3V_3 + I_{L_3} + I_{w_3}(V_3) &= 0,\\
\dot{I}_1 - \frac{V_1 - V_2}{L_0} &= 0,\\
\dot{I}_2 - \frac{V_2 - V_3}{L_0} &= 0,\\
\dot{I}_3 - \frac{V_3 - V_1}{L_0} &= 0,\\
\dot{I_{L_1}} - \frac{V_1}{L_1} &= 0,\\
\dot{I_{L_2}} - \frac{V_2}{L_2} &= 0,\\
\dot{I_{L_3}} - \frac{V_3}{L_3} &= 0.
\end{aligned}
\tag{2}
$$

We consider two cases of system (2) according to the equations describing memristors.

2.1. Case 1. In this case, the nonlinearities of the three memristors are described as follows:

$$q_{w_i}(\phi_i) = m_i\phi_i^3 - n_i\phi_i, \quad m_i, n_i > 0,\ i = 1, 2, 3. \tag{3}$$

By integrating both sides of each equation of system (2) between times t_0 and t while using (3) and the relations

$$q(t) = \int_{-\infty}^{t} I(u)\,du, \tag{4}$$

$$\phi(t) = \int_{-\infty}^{t} V(u)\,du, \tag{5}$$

we get

$$\dot{\phi}_1 + \frac{g_1\phi_1}{C_1} + \frac{q_{L_1}}{C_1} + \frac{m_1\phi_1^3}{C_1} - \frac{n_1\phi_1}{C_1} + \frac{q_1}{C_1} - \frac{q_3}{C_1} = 0, \quad (6)$$

$$\dot{\phi}_2 + \frac{g_2\phi_2}{C_2} + \frac{q_{L_2}}{C_2} + \frac{m_2\phi_2^3}{C_2} - \frac{n_2\phi_2}{C_2} - \frac{q_1}{C_2} + \frac{q_2}{C_2} = 0, \quad (7)$$

$$\dot{\phi}_3 + \frac{g_3\phi_3}{C_3} + \frac{q_{L_3}}{C_3} + \frac{m_3\phi_3^3}{C_3} - \frac{n_3\phi_3}{C_3} + \frac{q_3}{C_3} - \frac{q_2}{C_3} = 0, \quad (8)$$

$$\dot{q}_1 - \frac{\phi_1 - \phi_2}{L_0} = 0, \quad (9)$$

$$\dot{q}_2 - \frac{\phi_2 - \phi_3}{L_0} = 0, \quad (10)$$

$$\dot{q}_3 - \frac{\phi_3 - \phi_1}{L_0} = 0, \quad (11)$$

$$\dot{q_{L_1}} - \frac{\phi_1}{L_1} = 0, \quad (12)$$

$$\dot{q_{L_2}} - \frac{\phi_2}{L_2} = 0, \quad (13)$$

$$\dot{q_{L_3}} - \frac{\phi_3}{L_3} = 0. \quad (14)$$

By differentiating (6)–(8) and using (9)–(14), we obtain the following equations that depict our intended case:

$$\ddot{\phi}_j - \dot{\phi}_j\left(\frac{n_j - g_j}{C_j} - \frac{\left(3m_j\right)\phi_j^2}{C_j}\right) + \phi_j\left(\frac{1}{C_jL_j} + \frac{2}{C_jL_0}\right) - \frac{\sum_{k=1,k\neq j}^{3}\phi_k}{C_jL_0} = 0, \quad j = 1,2,3. \quad (15)$$

2.2. Case 2. In this case, the nonlinearities of the three memristors are different and described as follows:

$$q_{w_1}(\phi_1) = m_1\phi_1^3 - n_1\phi_1,$$
$$q_{w_2}(\phi_2) = h_2\phi_2^4 + m_2\phi_2^3 - n_2\phi_2,$$
$$q_{w_3}(\phi_3) = h_3\phi_3^4 - n_3\phi_3. \quad (16)$$
$$m_i, h_{i+1}, n_j > 0, \quad i = 1,2, \ j = 1,2,3.$$

Using the same procedure as in Section 2.1, we obtain

$$\ddot{\phi}_1 - \dot{\phi}_1\left(\frac{n_1 - g_1}{C_1} - \frac{\left(3m_1\right)\phi_1^2}{C_1}\right) + \phi_1\left(\frac{1}{C_1L_1} + \frac{2}{C_1L_0}\right) - \frac{\phi_2 + \phi_3}{C_1L_0} = 0,$$

$$\ddot{\phi}_2 - \dot{\phi}_2\left(\frac{n_2 - g_2}{C_2} - \frac{\left(3m_2\right)\phi_2^2}{C_2} - \frac{\left(4h_2\right)\phi_2^3}{C_2}\right) + \phi_2\left(\frac{1}{C_2L_2} + \frac{2}{C_2L_0}\right) - \frac{\phi_1 + \phi_3}{C_2L_0} = 0,$$

$$\ddot{\phi}_3 - \dot{\phi}_3\left(\frac{n_3 - g_3}{C_3} - \frac{\left(4h_3\right)\phi_3^3}{C_3}\right) + \phi_3\left(\frac{1}{C_3L_3} + \frac{2}{C_3L_0}\right) - \frac{\phi_2 + \phi_1}{C_3L_0} = 0. \quad (17)$$

3. Normal Forms

The purpose of this section is to acquire the normal forms corresponding to each case of ring model derived in previous section. The powerful perturbation techniques are used to achieve this goal. First, systems (15) and (17) are written in perturbed form; then each system is reduced to an equivalent first-order system [36].

System (15) can be written in perturbed form as follows:

$$\ddot{x}_j - \varepsilon\dot{x}_j\left(a_j - \alpha_j x_j^2\right) + \beta_j x_j - b_j\varepsilon\left(\sum_{k=1,k\neq j}^{3} x_k\right) = 0, \quad j = 1,2,3. \quad (18)$$

And system (17) can be written in perturbed form as follows:

$$\ddot{x}_1 - \varepsilon\dot{x}_1\left(a_1 - \alpha_1 x_1^2\right) + \beta_1 x_1 - b_1\varepsilon\left(x_2 + x_3\right) = 0,$$
$$\ddot{x}_2 - \varepsilon\dot{x}_2\left(a_2 - \alpha_3 x_2^3 - \alpha_2 x_2^2\right) + \beta_2 x_2 - b_2\varepsilon\left(x_1 + x_3\right) = 0,$$
$$\ddot{x}_3 - \varepsilon\dot{x}_3\left(a_3 - \alpha_4 x_3^3\right) + \beta_3 x_3 - b_3\varepsilon\left(x_1 + x_2\right) = 0. \quad (19)$$

By using the substitutions

$$x_j(t) = \overline{y_j}(t) + y_j(t),$$
$$\dot{x}_j(t) = i\sqrt{\beta_j}\left(y_j(t) - \overline{y_j(t)}\right), \quad j = 1,2,3, \quad (20)$$

where $\overline{y_j}(t)$ is the complex conjugate of $y_j(t)$, systems (18) and (19) are reduced to the more simplified first-order systems of DEs. More specifically, system (18) is reduced to the following system:

$$\dot{y}_j - \frac{1}{2}\varepsilon\left(y_j - \overline{y_j}\right)\left(a_j - \alpha_j\left(\overline{y_j} + y_j\right)^2\right) + \frac{\left(ib_j\right)\varepsilon\left(\sum_{k=1,k\neq j}^{3}\overline{y_{k0}} + y_{k0}\right)}{2\sqrt{\beta_j}} - i\sqrt{\beta_j}y_j = 0, \quad j = 1,2,3. \quad (21)$$

And system (19) is reduced to the following system:

$$\begin{aligned}
&\dot{y}_1 - \frac{1}{2}\varepsilon\left(y_1 - \overline{y_1}\right)\left(a_1 - \alpha_1\left(\overline{y_1} + y_1\right)^2\right) \\
&\quad + \frac{(ib_1)\,\varepsilon\left(\overline{y_2} + \overline{y_3} + y_2 + y_3\right)}{2\sqrt{\beta_1}} - i\sqrt{\beta_1}y_1 = 0, \\
&\dot{y}_2 - \frac{1}{2}\varepsilon\left(y_2 - \overline{y_2}\right) \\
&\quad \cdot\left(-\alpha_3\left(\overline{y_2} + y_2\right)^3 - \alpha_2\left(\overline{y_2} + y_2\right)^2 + a_2\right) \\
&\quad + \frac{(ib_2)\,\varepsilon\left(\overline{y_1} + \overline{y_3} + y_1 + y_3\right)}{2\sqrt{\beta_2}} - i\sqrt{\beta_2}y_2 = 0, \\
&\dot{y}_3 - \frac{1}{2}\varepsilon\left(y_3 - \overline{y_3}\right)\left(a_3 - \alpha_4\left(\overline{y_3} + y_3\right)^3\right) \\
&\quad + \frac{(ib_3)\,\varepsilon\left(\overline{y_1} + \overline{y_2} + y_1 + y_2\right)}{2\sqrt{\beta_3}} - i\sqrt{\beta_3}y_3 = 0.
\end{aligned} \tag{22}$$

The normal forms corresponding to systems (21) and (22) are obtained by applying the method of multiple scales [36].

3.1. The Normal Form of Case 1 of Ring Model. Using the substitutions

$$\begin{aligned}
y_j(t;\varepsilon) &= \sum_{k=0}^{2}\varepsilon^k y_{\mathrm{jk}}\left(T_0, T_1, T_2\right), \\
T_{j-1} &= \varepsilon^{j-1}t, \\
\frac{d}{dt} &= \sum_{k=0}^{2} D_k\varepsilon^k, \\
D_{j-1} &= \partial_{T_{j-1}}, \\
&\qquad j = 1, 2, 3,
\end{aligned} \tag{23}$$

in system (21) and equating coefficients of equal powers of ε, we obtain

(**Order** ε^0)

$$D_0 y_{j0} - i\sqrt{\beta_j}y_{j0} = 0, \quad j = 1, 2, 3. \tag{24}$$

(**Order** ε^1)

$$\begin{aligned}
&D_0 y_{j1} - i\sqrt{\beta_j}y_{j1} \\
&\quad = -D_1 y_{j0} + \frac{\left(-ib_j\right)\left(\sum_{k=1,k\neq j}^{3}\overline{y_{\mathrm{k0}}} + y_{\mathrm{k0}}\right)}{2\sqrt{\beta_j}} \\
&\quad + \frac{1}{2}\left(\overline{y_{j0}} - y_{j0}\right)\left(\alpha_j\left(\overline{y_{j0}} + y_{j0}\right)^2 - a_j\right), \\
&\qquad j = 1, 2, 3.
\end{aligned} \tag{25}$$

(**Order** ε^2)

$$\begin{aligned}
&D_0 y_{12} - i\sqrt{\beta_1}y_{12} = \frac{(-ib_1)\left(\overline{y_{21}} + \overline{y_{31}} + y_{21} + y_{31}\right)}{2\sqrt{\beta 1}} \\
&\quad - D_2 y_{10} - D_1 y_{11} \\
&\quad + \frac{1}{2}\left(y_{11}\left(\alpha_1\left(\overline{y_{10}}^2 - 2y_{10}\overline{y_{10}} - 3y_{10}^2\right) + a_1\right)\right. \\
&\quad \left. - \overline{y_{11}}\left(\alpha_1\left(-3\overline{y_{10}}^2 - 2y_{10}\overline{y_{10}} + y_{10}^2\right) + a_1\right)\right), \\
&D_0 y_{22} - i\sqrt{\beta_2}y_{22} = \frac{(-ib_2)\left(\overline{y_{11}} + \overline{y_{31}} + y_{11} + y_{31}\right)}{2\sqrt{\beta_2}} \\
&\quad - D_2 y_{20} - D_1 y_{21} \\
&\quad + \frac{1}{2}\left(y_{21}\left(\alpha_2\left(\overline{y_{20}}^2 - 2y_{20}\overline{y_{20}} - 3y_{20}^2\right) + a_2\right)\right. \\
&\quad \left. - \overline{y_{21}}\left(\alpha_2\left(-3\overline{y_{20}}^2 - 2y_{20}\overline{y_{20}} + y_{20}^2\right) + a_2\right)\right), \\
&D_0 y_{32} - i\sqrt{\beta_3}y_{32} = \frac{(-ib_3)\left(\overline{y_{11}} + \overline{y_{21}} + y_{11} + y_{21}\right)}{2\sqrt{\beta_3}} \\
&\quad - D_2 y_{30} - D_1 y_{31} \\
&\quad + \frac{1}{2}\left(y_{31}\left(\alpha_3\left(\overline{y_{30}}^2 - 2y_{30}\overline{y_{30}} - 3y_{30}^2\right) + a_3\right)\right. \\
&\quad \left. - \overline{y_{31}}\left(\alpha_3\left(-3\overline{y_{30}}^2 - 2y_{30}\overline{y_{30}} + y_{30}^2\right) + a_3\right)\right).
\end{aligned} \tag{26}$$

Solving system (24) of DEs we get

$$y_{j0} = e^{i\sqrt{\beta_j}T_0}A_{j0}\left(T_1, T_2\right), \quad j = 1, 2, 3. \tag{27}$$

By substituting these solutions in (25) we get the conditions needed to remove the secular terms in the following forms:

$$D_1 A_{j0} = \frac{a_j A_{j0}}{2} - \frac{1}{2}\alpha_j A_{j0}^2\overline{A_{j0}}, \quad j = 1, 2, 3. \tag{28}$$

Using (28) to solve system (25) and substituting from the results in (26), we get the following conditions to remove the secular terms

$$D_2 A_{10} = -\frac{iA_{10}\left(\left(\beta_1 - \beta_2\right)\left(\beta_1 - \beta_3\right)\left(-12\alpha_1 a_1 A_{10}\overline{A_{10}} + 11\alpha_1^2 A_{10}^2\overline{A_{10}}^2 + 2a_1^2\right) - 8b_1\left(b_3\left(\beta_1 - \beta_2\right) + b_2\left(\beta_1 - \beta_3\right)\right)\right)}{16\sqrt{\beta_1}\left(\beta_1 - \beta_2\right)\left(\beta_1 - \beta_3\right)},$$

$$D_2 A_{20} = \frac{iA_{20}\left(\left(\beta_1 - \beta_2\right)\left(\beta_2 - \beta_3\right)\left(-12\alpha_2 a_2 A_{20}\overline{A_{20}} + 11\alpha_2^2 A_{20}^2\overline{A_{20}}^2 + 2a_2^2\right) - 8b_2\left(b_3\left(\beta_1 - \beta_2\right) + b_1\left(\beta_3 - \beta_2\right)\right)\right)}{16\sqrt{\beta_2}\left(\beta_2 - \beta_1\right)\left(\beta_2 - \beta_3\right)},$$

$$D_2A_{30} = -\frac{iA_{30}\left(\left(\beta_2-\beta_3\right)\left(\left(\beta_1-\beta_3\right)\left(-12\alpha_3a_3A_{30}\overline{A_{30}}+11\alpha_3^2A_{30}^2\overline{A_{30}}^2+2a_3^2\right)+8b_1b_3\right)+8b_2b_3\left(\beta_1-\beta_3\right)\right)}{16\sqrt{\beta_3}\left(\beta_3-\beta_1\right)\left(\beta_3-\beta_2\right)}. \tag{29}$$

Substituting from (28) and (29) in $\dot{A_{j0}} = D_2\varepsilon^2A_{j0} + D_1\varepsilon A_{j0}$, where $j = 1, 2$ and 3, we obtain the normal form of system (21) which can be expressed in the following form:

$$\begin{aligned}
\dot{r_{j0}} &= \frac{1}{2}\varepsilon r_{j0}\left(a_j-\alpha_jr_{j0}^2\right), \quad j=1,2,3,\\
\dot{\theta_{10}} &= \frac{\varepsilon^2\left(8b_1\left(b_3\left(\beta_1-\beta_2\right)+b_2\left(\beta_1-\beta_3\right)\right)-\left(\beta_1-\beta_2\right)\left(\beta_1-\beta_3\right)\left(-12a_1\alpha_1r_{10}^2+2a_1^2+11\alpha_1^2r_{10}^4\right)\right)}{16\sqrt{\beta_1}\left(\beta_1-\beta_2\right)\left(\beta_1-\beta_3\right)},\\
\dot{\theta_{20}} &= -\frac{\varepsilon^2\left(8b_2\left(b_3\left(\beta_1-\beta_2\right)+b_1\left(\beta_3-\beta_2\right)\right)-\left(\beta_1-\beta_2\right)\left(\beta_2-\beta_3\right)\left(-12a_2\alpha_2r_{20}^2+2a_2^2+11\alpha_2^2r_{20}^4\right)\right)}{16\sqrt{\beta_2}\left(\beta_2-\beta_1\right)\left(\beta_2-\beta_3\right)},\\
\dot{\theta_{30}} &= -\frac{\varepsilon^2\left(\left(\beta_2-\beta_3\right)\left(\left(\beta_1-\beta_3\right)\left(-12a_3\alpha_3r_{30}^2+2a_3^2+11\alpha_3^2r_{30}^4\right)+8b_1b_3\right)+8b_2b_3\left(\beta_1-\beta_3\right)\right)}{16\sqrt{\beta_3}\left(\beta_3-\beta_1\right)\left(\beta_3-\beta_2\right)}.
\end{aligned} \tag{30}$$

3.2. The Normal Form of Case 2 of Ring Model. Using the same procedure applied in Section 3.1, the following conditions are obtained to remove the secular terms of order ε^1

$$\begin{aligned}
D_1A_{20} &= \frac{a_2A_{20}}{2}-\frac{1}{2}\alpha_2A_{20}^2\overline{A_{20}},\\
D_1A_{30} &= \frac{a_3A_{30}}{2},
\end{aligned} \tag{31}$$

$$D_1A_{10} = \frac{a_1A_{10}}{2}-\frac{1}{2}\alpha_1A_{10}^2\overline{A_{10}},$$

and the conditions needed to remove the secular terms of order ε^2 are given by

$$\begin{aligned}
D_2A_{10} &= -\frac{iA_{10}\left(\left(\beta_1-\beta_2\right)\left(-12\alpha_1a_1A_{10}\overline{A_{10}}+11\alpha_1^2A_{10}^2\overline{A_{10}}^2+2a_1^2\right)-8b_1b_2\right)}{16\sqrt{\beta_1}\left(\beta_1-\beta_2\right)},\\
D_2A_{20} &= \frac{iA_{20}\left(\left(\beta_1-\beta_2\right)\left(-60\alpha_2a_2A_{20}\overline{A_{20}}+A_{20}^2\overline{A_{20}}^2\left(56\alpha_3^2A_{20}\overline{A_{20}}+55\alpha_2^2\right)+10a_2^2\right)+40b_1b_2\right)}{80\sqrt{\beta_2}\left(\beta_2-\beta_1\right)},\\
D_2A_{30} &= \frac{iA_{30}\left(\left(\beta_2-\beta_3\right)\left(-a_3\left(\beta_1-\beta_3\right)\left(a_3-\alpha_3A_{30}\overline{A_{30}}\right)-4b_1b_3\right)+4b_2b_3\left(\beta_3-\beta_1\right)\right)}{8\sqrt{\beta_3}\left(\beta_3-\beta_1\right)\left(\beta_3-\beta_2\right)}.
\end{aligned} \tag{32}$$

So, we get the following normal form:

$$\begin{aligned}
\dot{r_{10}} &= \frac{1}{2}\varepsilon r_{10}\left(a_1-\alpha_1r_{10}^2\right),\\
\dot{r_{20}} &= \frac{1}{2}\varepsilon r_{20}\left(a_2-\alpha_2r_{20}^2\right),\\
\dot{r_{30}} &= \frac{1}{2}a_3\varepsilon r_{30},\\
\dot{\theta_{10}} &= \frac{\varepsilon^2\left(8b_1b_2-\left(\beta_1-\beta_2\right)\left(-12a_1\alpha_1r_{10}^2+2a_1^2+11\alpha_1^2r_{10}^4\right)\right)}{16\sqrt{\beta_1}\left(\beta_1-\beta_2\right)},
\end{aligned}$$

$$\dot{\theta_{20}} = \frac{\varepsilon^2\left(\left(\beta_1-\beta_2\right)\left(-60a_2\alpha_2r_{20}^2+10a_2^2+56\alpha_3^2r_{20}^6+55\alpha_2^2r_{20}^4\right)+40b_1b_2\right)}{80\sqrt{\beta_2}\left(\beta_2-\beta_1\right)},$$

$$\dot{\theta_{30}} = -\frac{\varepsilon^2\left(\left(\beta_2-\beta_3\right)\left(a_3\left(\beta_1-\beta_3\right)\left(a_3-\alpha_3r_{30}^2\right)+4b_1b_3\right)+4b_2b_3\left(\beta_1-\beta_3\right)\right)}{8\sqrt{\beta_3}\left(\beta_3-\beta_1\right)\left(\beta_3-\beta_2\right)}. \tag{33}$$

4. Stability Analysis of Equilibrium Solutions

In this section, the stability analysis of the equilibrium solutions is carried out using the normal forms obtained in (30) and (33).

4.1. Stability Analysis of Case 1 of Ring Model. The Jacobian matrix of system (30) is expressed as

$$J = \begin{pmatrix} \frac{1}{2}\varepsilon\left(a_1-r_{10}^2\alpha_1\right)-\varepsilon r_{10}^2\alpha_1 & 0 & 0 \\ 0 & \frac{1}{2}\varepsilon\left(a_2-r_{20}^2\alpha_2\right)-\varepsilon r_{20}^2\alpha_2 & 0 \\ 0 & 0 & \frac{1}{2}\varepsilon\left(a_3-r_{30}^2\alpha_3\right)-\varepsilon r_{30}^2\alpha_3 \end{pmatrix}. \tag{34}$$

System (30) has the following equilibrium solutions.

4.1.1. Equilibrium Point. The following equilibrium solution,

$$r_{i0} = 0, \quad i = 1,2,3, \tag{35}$$

is corresponding to an equilibrium point at origin. Evaluating the eigenvalues of Jacobian matrix (34) at equilibrium point (35), we get the stability region of this point in parameters space as follows:

$$\begin{aligned} a_1 &< 0, \\ a_2 &< 0, \\ a_3 &< 0. \end{aligned} \tag{36}$$

4.1.2. Periodic Solution I. The second equilibrium solution,

$$\begin{aligned} r_{10} &= 0, \\ r_{20} &= 0, \\ r_{30} &= \sqrt{\frac{a_3}{\alpha_3}}, \\ \dot{\theta_{30}} &= -\frac{\varepsilon^2\left(\left(\beta_2-\beta_3\right)\left(\left(\beta_1-\beta_3\right)\left(-12a_3\alpha_3r_{30}^2+2a_3^2+11\alpha_3^2r_{30}^4\right)+8b_1b_3\right)+8b_2b_3\left(\beta_1-\beta_3\right)\right)}{16\sqrt{\beta_3}\left(\beta_3-\beta_1\right)\left(\beta_3-\beta_2\right)}, \end{aligned} \tag{37}$$

corresponds to a periodic solution in the phase space of case 1 of ladder model. The second order approximate solution of this periodic orbit has an amplitude given by $\sqrt{a_3/\alpha_3}$ and an angular frequency computed as

$$\sqrt{\beta_3} - \frac{\varepsilon^2\left(\left(\beta_2-\beta_3\right)\left(a_3^2\left(\beta_1-\beta_3\right)+8b_1b_3\right)+8b_2b_3\left(\beta_1-\beta_3\right)\right)}{16\sqrt{\beta_3}\left(\beta_3-\beta_1\right)\left(\beta_3-\beta_2\right)}. \tag{38}$$

Evaluating the eigenvalues of Jacobian matrix (34) at periodic solution I (37), we get its stability region in parameters space as follows:

$$\begin{aligned} a_1 &< 0, \\ a_2 &< 0, \\ a_3 &> 0. \end{aligned} \tag{39}$$

4.1.3. Periodic Solution II. The third equilibrium solution,

$$\begin{aligned} r_{10} &= 0, \\ r_{20} &= \sqrt{\frac{a_2}{\alpha_2}}, \\ r_{30} &= 0, \\ \dot{\theta_{20}} &= -\frac{\varepsilon^2\left(8b_2\left(b_3\left(\beta_1-\beta_2\right)+b_1\left(\beta_3-\beta_2\right)\right)-\left(\beta_1-\beta_2\right)\left(\beta_2-\beta_3\right)\left(-12a_2\alpha_2r_{20}^2+2a_2^2+11\alpha_2^2r_{20}^4\right)\right)}{16\sqrt{\beta_2}\left(\beta_2-\beta_1\right)\left(\beta_2-\beta_3\right)}, \end{aligned} \tag{40}$$

represents a periodic solution in the phase space of case 1 of ring model. The second order approximate solution of this periodic orbit has an amplitude given by $\sqrt{a_2/\alpha_2}$ and an angular frequency computed as

$$\sqrt{\beta_2}-\frac{\varepsilon^2\left(8b_2\left(b_3\left(\beta_1-\beta_2\right)+b_1\left(\beta_3-\beta_2\right)\right)-a_2^2\left(\beta_1-\beta_2\right)\left(\beta_2-\beta_3\right)\right)}{16\sqrt{\beta_2}\left(\beta_2-\beta_1\right)\left(\beta_2-\beta_3\right)}. \tag{41}$$

Evaluating the eigenvalues of Jacobian matrix (34) at periodic solution II (40), we get its stability region in parameters space as follows:

$$\begin{aligned} a_2 &> 0, \\ a_3 &< 0. \end{aligned} \tag{42}$$

$$a_1 < 0,$$

4.1.4. Periodic Solution III. The fourth equilibrium solution,

$$\begin{aligned} r_{10} &= \sqrt{\frac{a_1}{\alpha_1}}, \\ r_{20} &= 0, \\ r_{30} &= 0, \\ \dot{\theta_{10}} &= \frac{\varepsilon^2\left(8b_1\left(b_3\left(\beta_1-\beta_2\right)+b_2\left(\beta_1-\beta_3\right)\right)-\left(\beta_1-\beta_2\right)\left(\beta_1-\beta_3\right)\left(-12a_1\alpha_1r_{10}^2+2a_1^2+11\alpha_1^2r_{10}^4\right)\right)}{16\sqrt{\beta_1}\left(\beta_1-\beta_2\right)\left(\beta_1-\beta_3\right)}, \end{aligned} \tag{43}$$

corresponds to a periodic solution in the phase space of case 1 of ring model. The second order approximate solution of this periodic orbit has an amplitude given by $\sqrt{a_1/\alpha_1}$ and an angular frequency computed as

$$\sqrt{\beta_1}+\frac{\varepsilon^2\left(8b_1\left(b_3\left(\beta_1-\beta_2\right)+b_2\left(\beta_1-\beta_3\right)\right)-a_1^2\left(\beta_1-\beta_2\right)\left(\beta_1-\beta_3\right)\right)}{16\sqrt{\beta_1}\left(\beta_1-\beta_2\right)\left(\beta_1-\beta_3\right)}. \tag{44}$$

Evaluating the eigenvalues of Jacobian matrix (34) at periodic solution III (43), we get its stability region in parameters space as follows:

$$\begin{aligned} a_2 &< 0, \\ a_3 &< 0. \end{aligned} \tag{45}$$

$$a_1 > 0,$$

4.1.5. 2D Torus I. The fifth equilibrium solution,

$$
\begin{aligned}
r_{10} &= \sqrt{\frac{a_1}{\alpha_1}},\\
r_{20} &= \sqrt{\frac{a_2}{\alpha_2}},\\
r_{30} &= 0,\\
\dot{\theta_{10}} &= \frac{\varepsilon^2\left(8b_1\left(b_3\left(\beta_1-\beta_2\right)+b_2\left(\beta_1-\beta_3\right)\right)-\left(\beta_1-\beta_2\right)\left(\beta_1-\beta_3\right)\left(-12a_1\alpha_1r_{10}^2+2a_1^2+11\alpha_1^2r_{10}^4\right)\right)}{16\sqrt{\beta_1}\left(\beta_1-\beta_2\right)\left(\beta_1-\beta_3\right)},\\
\dot{\theta_{20}} &= -\frac{\varepsilon^2\left(8b_2\left(b_3\left(\beta_1-\beta_2\right)+b_1\left(\beta_3-\beta_2\right)\right)-\left(\beta_1-\beta_2\right)\left(\beta_2-\beta_3\right)\left(-12a_2\alpha_2r_{20}^2+2a_2^2+11\alpha_2^2r_{20}^4\right)\right)}{16\sqrt{\beta_2}\left(\beta_2-\beta_1\right)\left(\beta_2-\beta_3\right)},
\end{aligned}
\tag{46}
$$

corresponds to a 2D torus in the phase space of case 1 of ring model. The second order approximate solution of this 2D torus has two fundamental angular frequencies given by (44) and (41). Evaluating the eigenvalues of Jacobian matrix (34) at 2D torus I (46), we get the stability region in parameters space as follows:

$$
\begin{aligned}
a_1 &> 0,\\
a_2 &> 0,\\
a_3 &< 0.
\end{aligned}
\tag{47}
$$

4.1.6. 2D Torus II. The sixth equilibrium solution,

$$
\begin{aligned}
r_{10} &= \sqrt{\frac{a_1}{\alpha_1}},\\
r_{20} &= 0,\\
r_{30} &= \sqrt{\frac{a_3}{\alpha_3}},\\
\dot{\theta_{10}} &= \frac{\varepsilon^2\left(8b_1\left(b_3\left(\beta_1-\beta_2\right)+b_2\left(\beta_1-\beta_3\right)\right)-\left(\beta_1-\beta_2\right)\left(\beta_1-\beta_3\right)\left(-12a_1\alpha_1r_{10}^2+2a_1^2+11\alpha_1^2r_{10}^4\right)\right)}{16\sqrt{\beta_1}\left(\beta_1-\beta_2\right)\left(\beta_1-\beta_3\right)},\\
\dot{\theta_{30}} &= -\frac{\varepsilon^2\left(\left(\beta_2-\beta_3\right)\left(\left(\beta_1-\beta_3\right)\left(-12a_3\alpha_3r_{30}^2+2a_3^2+11\alpha_3^2r_{30}^4\right)+8b_1b_3\right)+8b_2b_3\left(\beta_1-\beta_3\right)\right)}{16\sqrt{\beta_3}\left(\beta_3-\beta_1\right)\left(\beta_3-\beta_2\right)},
\end{aligned}
\tag{48}
$$

corresponds to a 2D torus in the phase space of case 1 of ring model. The second order approximate solution of this 2D torus has two fundamental angular frequencies given by (44) and (38). Evaluating the eigenvalues of Jacobian matrix (34) at 2D torus II (48), we get the stability region in parameters space as follows:

$$
\begin{aligned}
a_1 &> 0,\\
a_2 &< 0,\\
a_3 &> 0.
\end{aligned}
\tag{49}
$$

4.1.7. 2D Torus III. The seventh equilibrium solution,

$$
\begin{aligned}
r_{10} &= 0,\\
r_{20} &= \sqrt{\frac{a_2}{\alpha_2}},
\end{aligned}
$$

$$
\begin{aligned}
r_{30} &= \sqrt{\frac{a_3}{\alpha_3}},\\
\dot{\theta_{20}} &= -\frac{\varepsilon^2\left(8b_2\left(b_3\left(\beta_1-\beta_2\right)+b_1\left(\beta_3-\beta_2\right)\right)-\left(\beta_1-\beta_2\right)\left(\beta_2-\beta_3\right)\left(-12a_2\alpha_2r_{20}^2+2a_2^2+11\alpha_2^2r_{20}^4\right)\right)}{16\sqrt{\beta_2}\left(\beta_2-\beta_1\right)\left(\beta_2-\beta_3\right)},\\
\dot{\theta_{30}} &= -\frac{\varepsilon^2\left(\left(\beta_2-\beta_3\right)\left(\left(\beta_1-\beta_3\right)\left(-12a_3\alpha_3r_{30}^2+2a_3^2+11\alpha_3^2r_{30}^4\right)+8b_1b_3\right)+8b_2b_3\left(\beta_1-\beta_3\right)\right)}{16\sqrt{\beta_3}\left(\beta_3-\beta_1\right)\left(\beta_3-\beta_2\right)},
\end{aligned}
\tag{50}
$$

corresponds to a 2D torus in the phase space of case 1 of ring model. The second order approximate solution of this 2D torus has two fundamental angular frequencies given by (41) and (38). Evaluating the eigenvalues of Jacobian matrix (34) at 2D torus III (50), we get the stability region in parameters space as follows:

$$
\begin{aligned}
a_1 &< 0,\\
a_2 &> 0,\\
a_3 &> 0.
\end{aligned}
\tag{51}
$$

4.1.8. 3D Torus. The eighth equilibrium solution,

$$
\begin{aligned}
r_{10} &= \sqrt{\frac{a_1}{\alpha_1}},\\
r_{20} &= \sqrt{\frac{a_2}{\alpha_2}},\\
r_{30} &= \sqrt{\frac{a_3}{\alpha_3}},\\
\dot{\theta_{10}} &= \frac{\varepsilon^2\left(8b_1\left(b_3\left(\beta_1-\beta_2\right)+b_2\left(\beta_1-\beta_3\right)\right)-\left(\beta_1-\beta_2\right)\left(\beta_1-\beta_3\right)\left(-12a_1\alpha_1r_{10}^2+2a_1^2+11\alpha_1^2r_{10}^4\right)\right)}{16\sqrt{\beta_1}\left(\beta_1-\beta_2\right)\left(\beta_1-\beta_3\right)},\\
\dot{\theta_{20}} &= -\frac{\varepsilon^2\left(8b_2\left(b_3\left(\beta_1-\beta_2\right)+b_1\left(\beta_3-\beta_2\right)\right)-\left(\beta_1-\beta_2\right)\left(\beta_2-\beta_3\right)\left(-12a_2\alpha_2r_{20}^2+2a_2^2+11\alpha_2^2r_{20}^4\right)\right)}{16\sqrt{\beta_2}\left(\beta_2-\beta_1\right)\left(\beta_2-\beta_3\right)},\\
\dot{\theta_{30}} &= -\frac{\varepsilon^2\left(\left(\beta_2-\beta_3\right)\left(\left(\beta_1-\beta_3\right)\left(-12a_3\alpha_3r_{30}^2+2a_3^2+11\alpha_3^2r_{30}^4\right)+8b_1b_3\right)+8b_2b_3\left(\beta_1-\beta_3\right)\right)}{16\sqrt{\beta_3}\left(\beta_3-\beta_1\right)\left(\beta_3-\beta_2\right)},
\end{aligned}
\tag{52}
$$

corresponds to a 3D torus in the phase space of case 1 of ring model. The second order approximate solution of this 3D torus has three fundamental angular frequencies given by (44), (41), and (38). Evaluating the eigenvalues of Jacobian matrix (34) at 3D torus (52), we get the stability region in parameters space as follows:

$$
\begin{aligned}
a_1 &> 0,\\
a_2 &> 0,\\
a_3 &> 0.
\end{aligned}
\tag{53}
$$

4.2. Stability Analysis of Case 2 of Ring Model. The Jacobian matrix of system (33) is given by

$$
\begin{pmatrix}
\frac{1}{2}\left(a_1-r_{10}^2\alpha_1\right)\varepsilon-r_{10}^2\alpha_1\varepsilon & 0 & 0\\
0 & \frac{1}{2}\left(a_2-r_{20}^2\alpha_2\right)\varepsilon-r_{20}^2\alpha_2\varepsilon & 0\\
0 & 0 & \frac{a_3\varepsilon}{2}
\end{pmatrix}.
\tag{54}
$$

System (33) has the following equilibrium solutions.

4.2.1. Equilibrium Point. The equilibrium solution

$$
r_{i0} = 0, \quad i = 1, 2, 3,
\tag{55}
$$

constitutes an equilibrium point at origin for case 2 of ring model. Evaluating the eigenvalues of Jacobian matrix (54) at

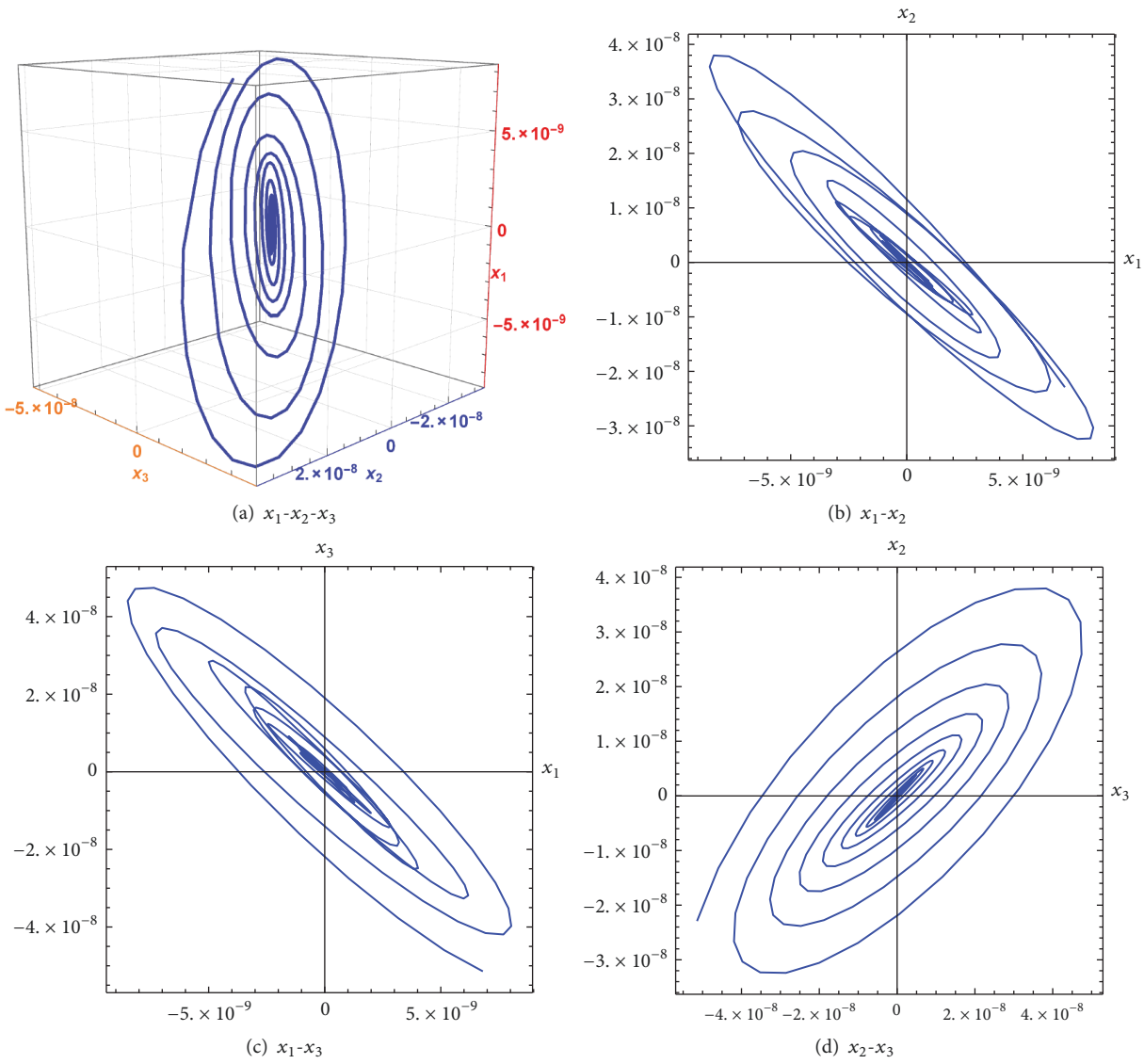

FIGURE 3: A stable equilibrium point of case 1 of ring model obtained when $\varepsilon = 0.1$, $a_1 = -1$, $a_2 = -0.5$, $a_3 = -1$, $\beta_1 = 1$, $\beta_2 = 2$, $\beta_3 = 2$, and $b_1 = b_2 = b_3 = \alpha_1 = \alpha_2 = \alpha_3 = 1$ in system (18).

equilibrium point (55), we get the following region of stability in parameters space:

$$\begin{aligned} &a_1 < 0, \\ &a_2 < 0, \\ &a_3 < 0. \end{aligned} \tag{56}$$

4.2.2. Periodic Solution I. The equilibrium solution,

$$\begin{aligned} r_{10} &= 0, \\ r_{20} &= \sqrt{\frac{a_2}{\alpha_2}}, \\ r_{30} &= 0, \\ \dot{\theta_{20}} &= \frac{\varepsilon^2 \left((\beta_1 - \beta_2) \left(-60 a_2 \alpha_2 r_{20}^2 + 10 a_2^2 + 56 \alpha_3^2 r_{20}^6 + 55 \alpha_2^2 r_{20}^4 \right) + 40 b_1 b_2 \right)}{80 \sqrt{\beta_2} (\beta_2 - \beta_1)}, \end{aligned} \tag{57}$$

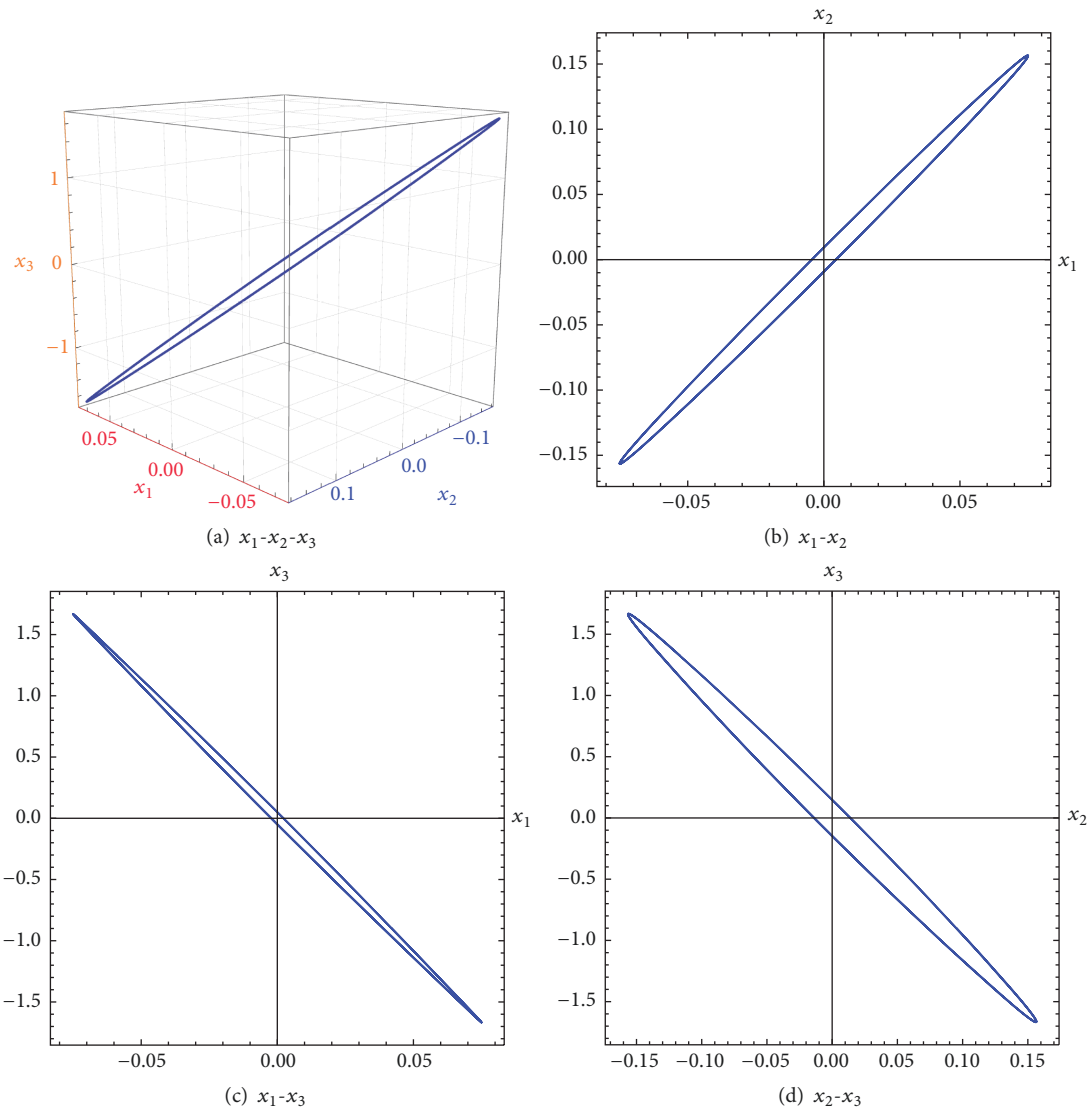

FIGURE 4: A stable periodic orbit of case 1 of ring model obtained when $\varepsilon = 0.1$, $a_1 = -0.4$, $a_2 = -0.5$, $a_3 = 0.7$, $\beta_1 = 1$, $\beta_2 = 2$, $\beta_3 = 3$, and $b_1 = b_2 = b_3 = \alpha_1 = \alpha_2 = \alpha_3 = 1$ in system (18).

constitutes a periodic solution in the phase space of case 2 of ring model. The second order approximate solution of this periodic orbit has an amplitude $\sqrt{a_2/\alpha_2}$ and an angular frequency given as

$$\sqrt{\beta_2} + \frac{\varepsilon^2\left(a_2^2\left(\beta_1-\beta_2\right)\left(56a_2\alpha_3^2+5\alpha_2^3\right)+40\alpha_2^3b_1b_2\right)}{80\alpha_2^3\sqrt{\beta_2}\left(\beta_2-\beta_1\right)}. \quad (58)$$

Evaluating the eigenvalues of Jacobian matrix (54) at periodic solution I (57), we get its stability region in parameters space as follows:

$$\begin{aligned} a_1 &< 0, \\ a_2 &> 0, \\ a_3 &< 0. \end{aligned} \quad (59)$$

4.2.3. Periodic Solution II. The equilibrium solution,

$$\begin{aligned} r_{10} &= \sqrt{\frac{a_1}{\alpha_1}}, \\ r_{20} &= 0, \\ r_{30} &= 0, \\ \dot{\theta}_{10} &= \frac{\varepsilon^2\left(8b_1b_2-\left(\beta_1-\beta_2\right)\left(-12a_1\alpha_1r_{10}^2+2a_1^2+11\alpha_1^2r_{10}^4\right)\right)}{16\sqrt{\beta_1}\left(\beta_1-\beta_2\right)}, \end{aligned} \quad (60)$$

constitutes a periodic solution in case 2 of ring model phase space. The second order approximate solution of this periodic orbit has an amplitude $\sqrt{a_1/\alpha_1}$ and an angular frequency given as

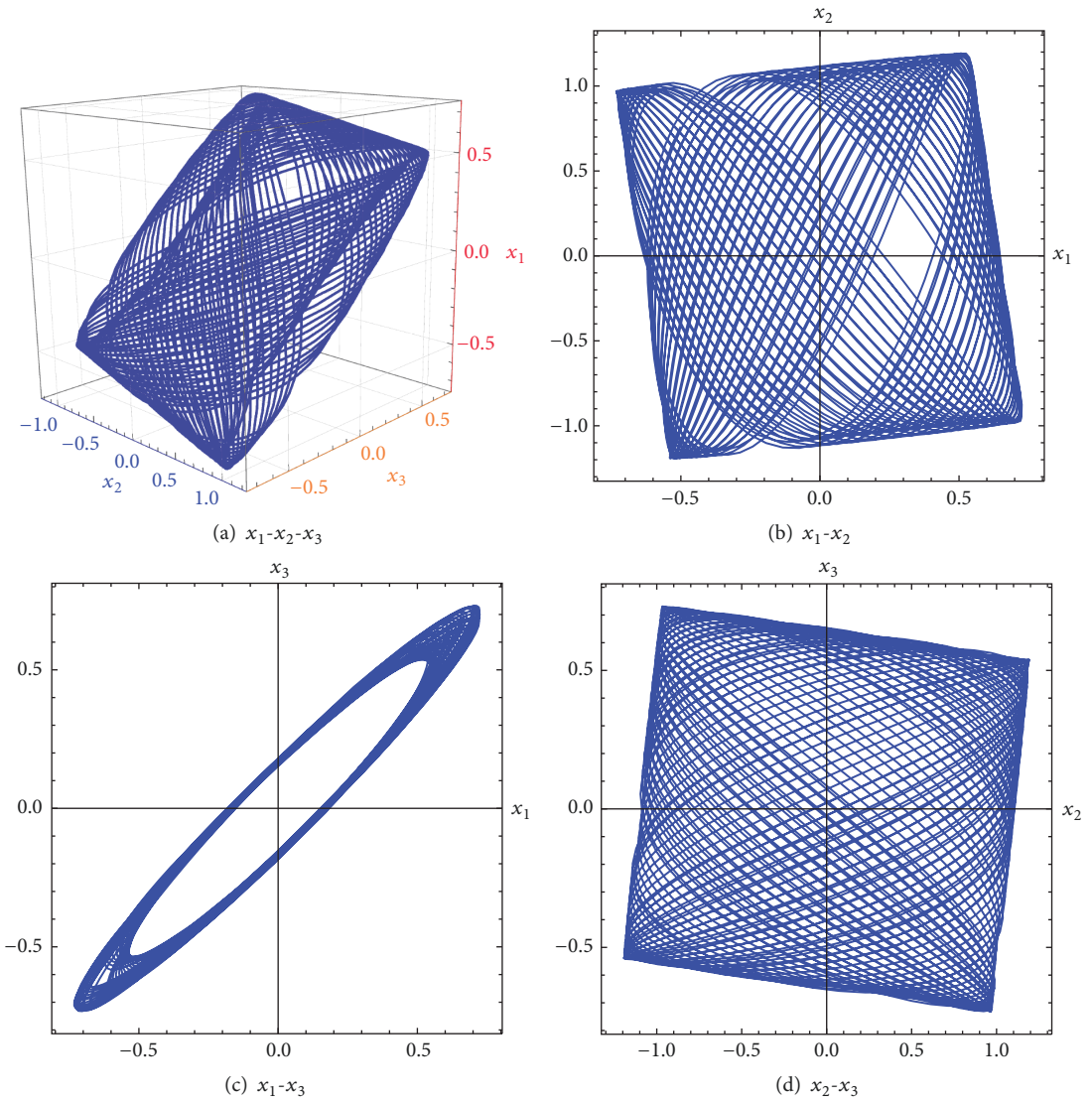

FIGURE 5: A stable 2D torus of case 1 of ring model obtained when $\varepsilon = 0.1$, $a_1 = 0.42$, $a_2 = 0.3$, $a_3 = -0.2$, $\beta_1 = 1$, $\beta_2 = 2$, $\beta_3 = 1$, and $b_1 = b_2 = b_3 = \alpha_1 = \alpha_2 = \alpha_3 = 1$ in system (18).

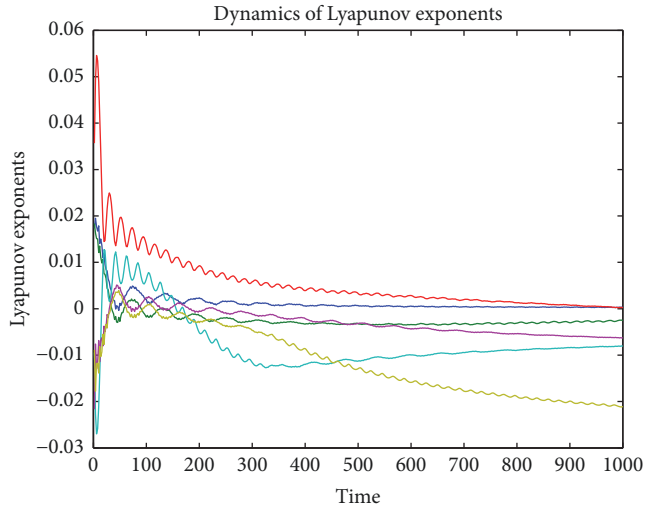

FIGURE 6: Lyapunov exponents of the equilibrium solution in Figure 5.

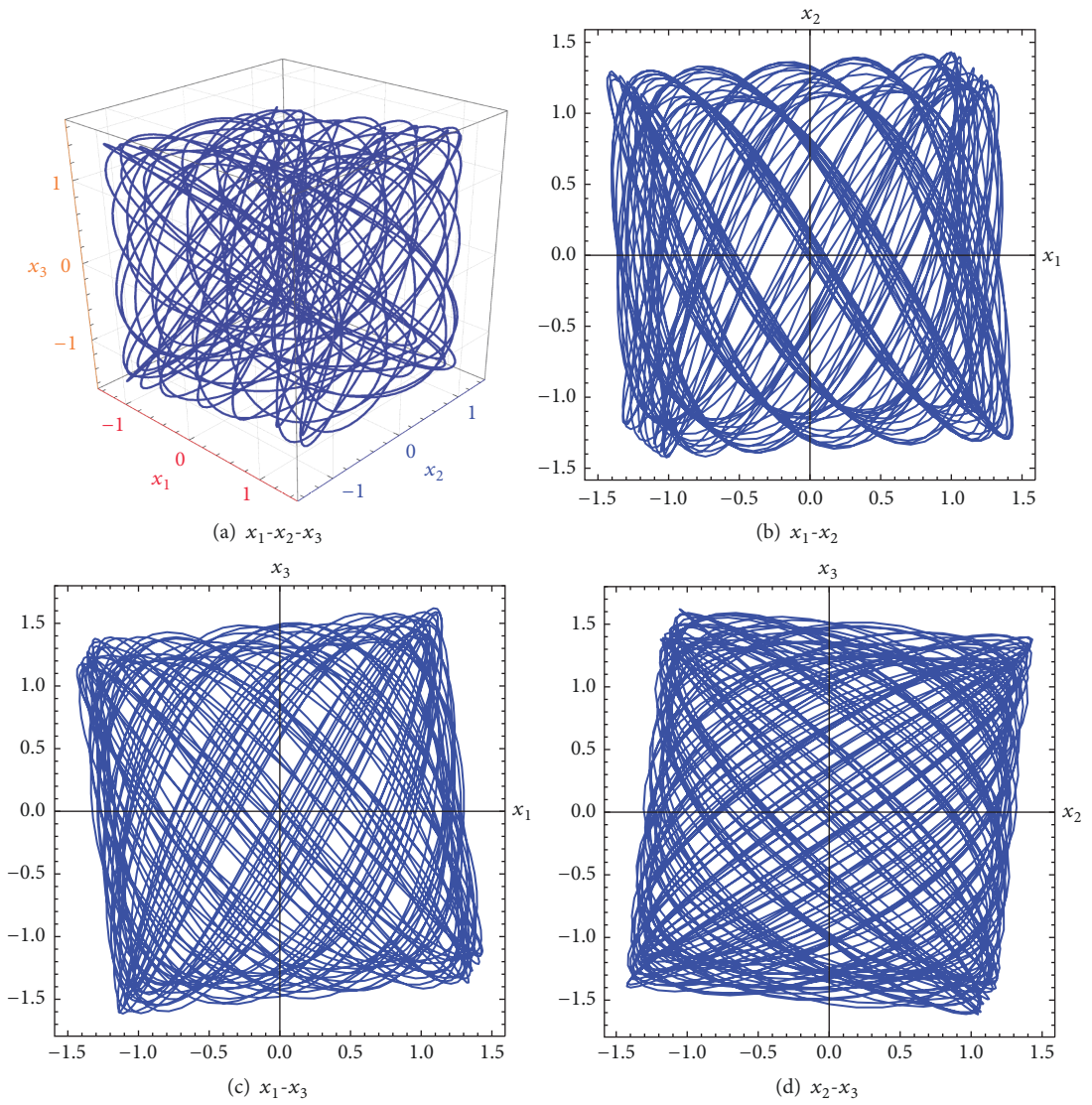

FIGURE 7: A stable 3D torus of case 1 of ring model obtained when $\varepsilon = 0.1$, $a_1 = 0.4$, $a_2 = 0.4$, $a_3 = 0.5$, $\beta_1 = 1$, $\beta_2 = 3$, $\beta_3 = 2$, and $b_1 = b_2 = b_3 = \alpha_1 = \alpha_2 = \alpha_3 = 1$ in system (18).

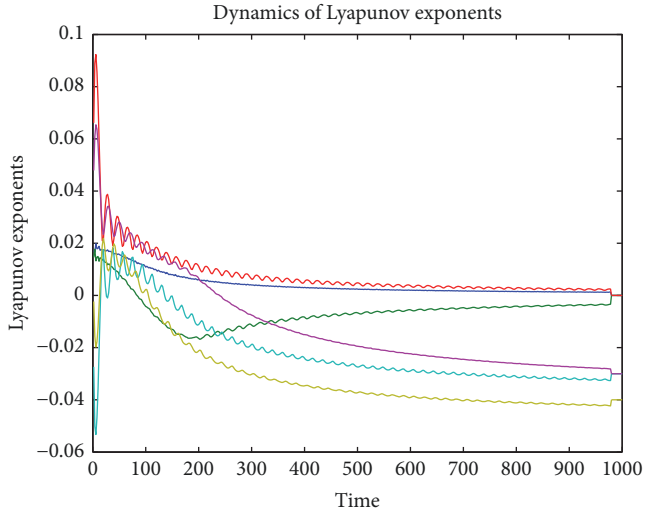

FIGURE 8: Lyapunov exponents of the equilibrium solution in Figure 7.

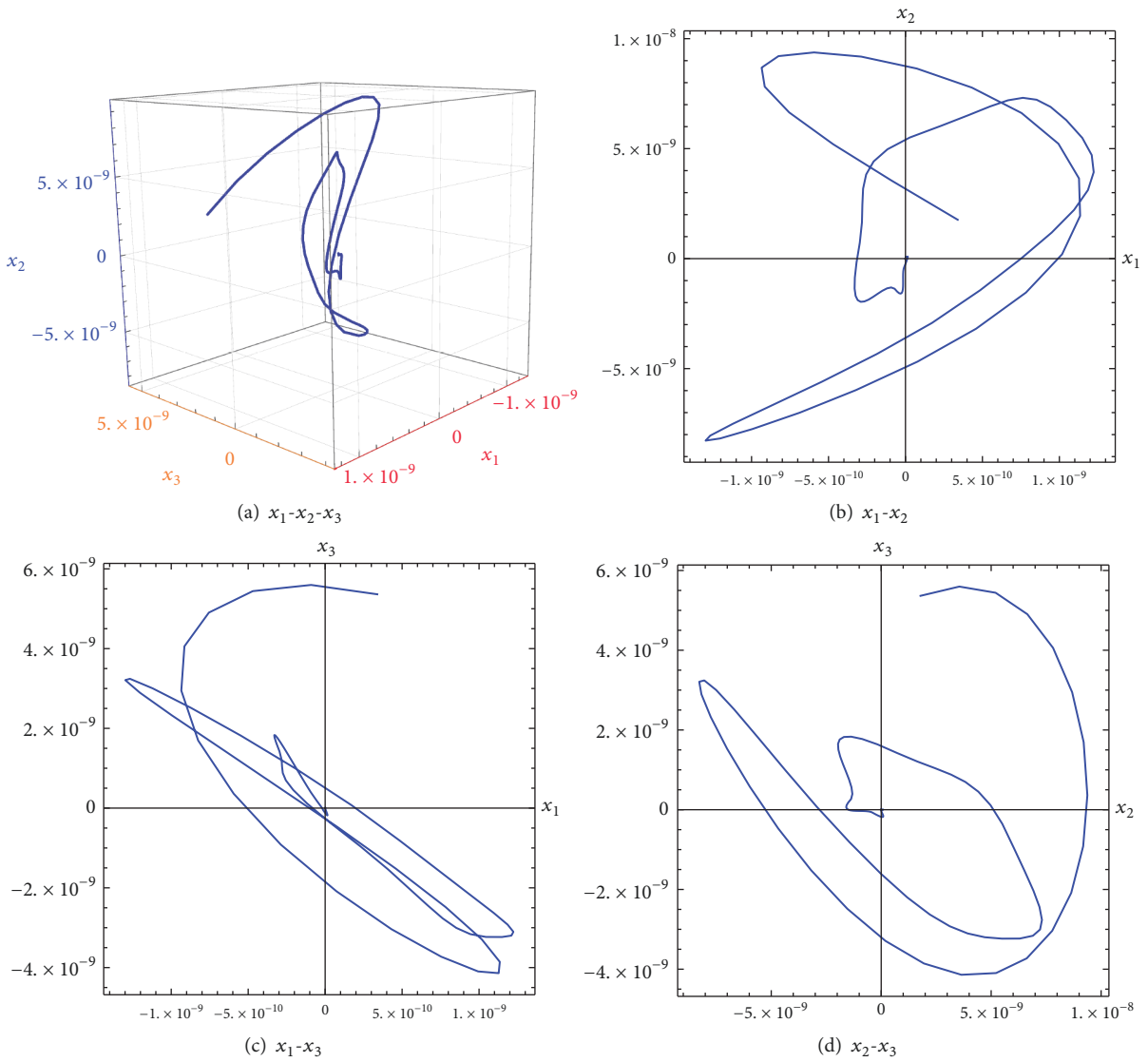

FIGURE 9: A stable equilibrium point of case 2 of ring model obtained when $\varepsilon = 0.1$, $a_1 = -1$, $a_2 = -1$, $a_3 = -1$, $\beta_1 = 3$, $\beta_2 = 1$, $\beta_3 = 2$, and $b_1 = b_2 = b_3 = \alpha_1 = \alpha_2 = \alpha_3 = \alpha_4 = 1$ in system (19).

$$\sqrt{\beta_1} + \frac{\varepsilon^2\left(a_1^2\left(\beta_2 - \beta_1\right) + 8b_1b_2\right)}{16\sqrt{\beta_1}\left(\beta_1 - \beta_2\right)}. \tag{61}$$

Evaluating the eigenvalues of Jacobian matrix (54) at periodic solution II (60), we get its stability region in parametric space as follows:

$$\begin{aligned} a_1 &> 0, \\ a_2 &< 0, \\ a_3 &< 0. \end{aligned} \tag{62}$$

4.2.4. 2D Torus. The equilibrium solution,

$$\begin{aligned} r_{10} &= \sqrt{\frac{a_1}{\alpha_1}}, \\ r_{20} &= \sqrt{\frac{a_2}{\alpha_2}}, \\ r_{30} &= 0, \end{aligned}$$

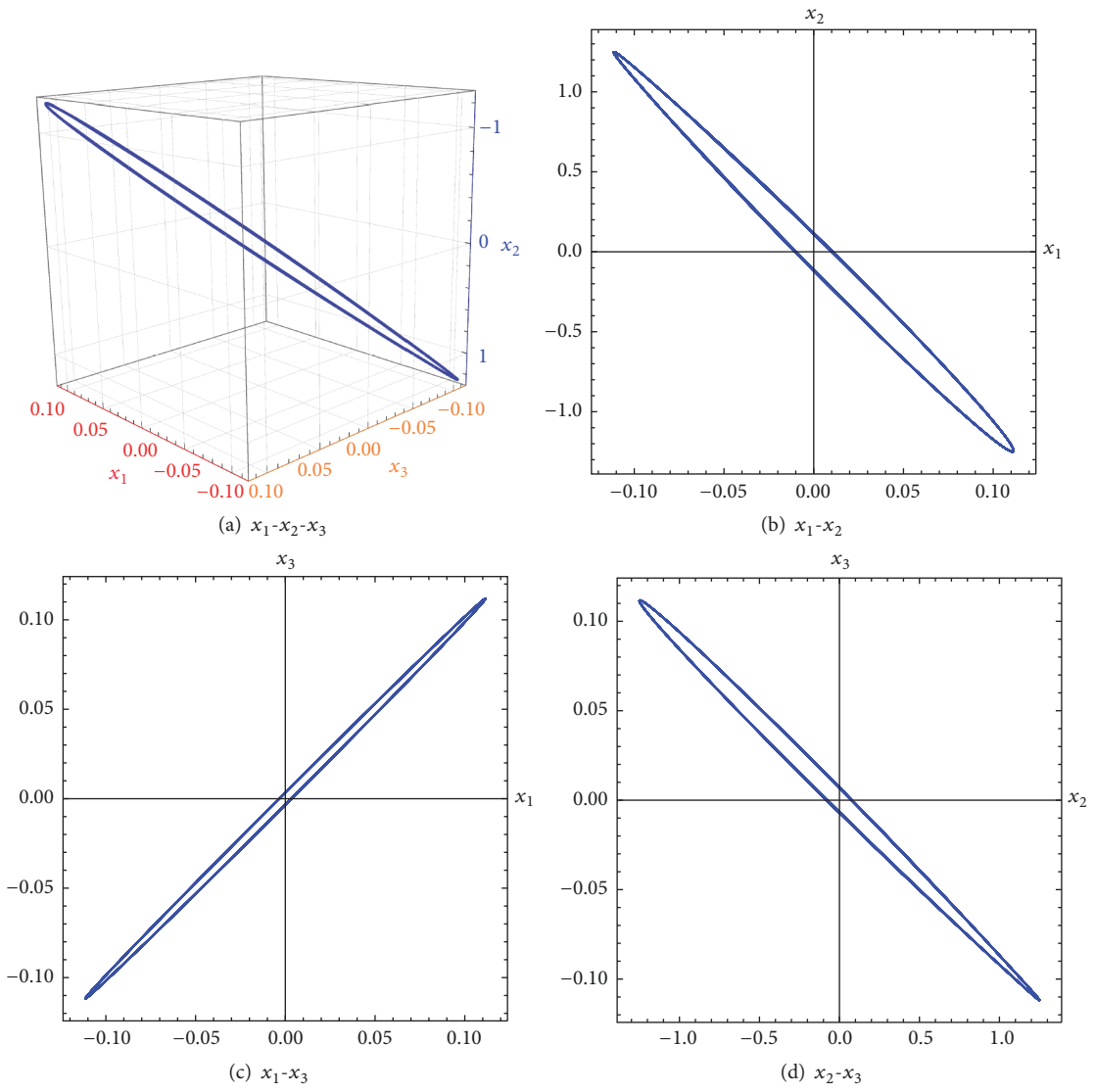

FIGURE 10: A stable periodic orbit of case 2 of ring model obtained when $\varepsilon = 0.1$, $a_1 = -0.7$, $a_2 = 0.4$, $a_3 = -0.5$, $\beta_1 = 1$, $\beta_2 = 2$, $\beta_3 = 1$, and $b_1 = b_2 = b_3 = \alpha_1 = \alpha_2 = \alpha_3 = \alpha_4 = 1$ in system (19).

$$\dot{\theta_{10}} = \frac{\varepsilon^2\left(8b_1b_2 - (\beta_1-\beta_2)\left(-12a_1\alpha_1r_{10}^2 + 2a_1^2 + 11\alpha_1^2r_{10}^4\right)\right)}{16\sqrt{\beta_1}\,(\beta_1-\beta_2)},$$

$$\dot{\theta_{20}} = \frac{\varepsilon^2\left((\beta_1-\beta_2)\left(-60a_2\alpha_2r_{20}^2 + 10a_2^2 + 56\alpha_3^2r_{20}^6 + 55\alpha_2^2r_{20}^4\right) + 40b_1b_2\right)}{80\sqrt{\beta_2}\,(\beta_2-\beta_1)}, \tag{63}$$

corresponds to a 2D torus in the phase space of case 2 of ring model. The second order approximate solution of this 2D torus has two fundamental angular frequencies given by (61) and (58). Evaluating the eigenvalues of Jacobian matrix (54) at 2D torus (63), we get the following stability region in parametric space:

$$\begin{aligned} a_1 &> 0, \\ a_2 &> 0, \\ a_3 &< 0. \end{aligned} \tag{64}$$

5. Numerical Simulations

In this section, numerical simulations are carried out to verify the theoretical results obtained in Section 4.

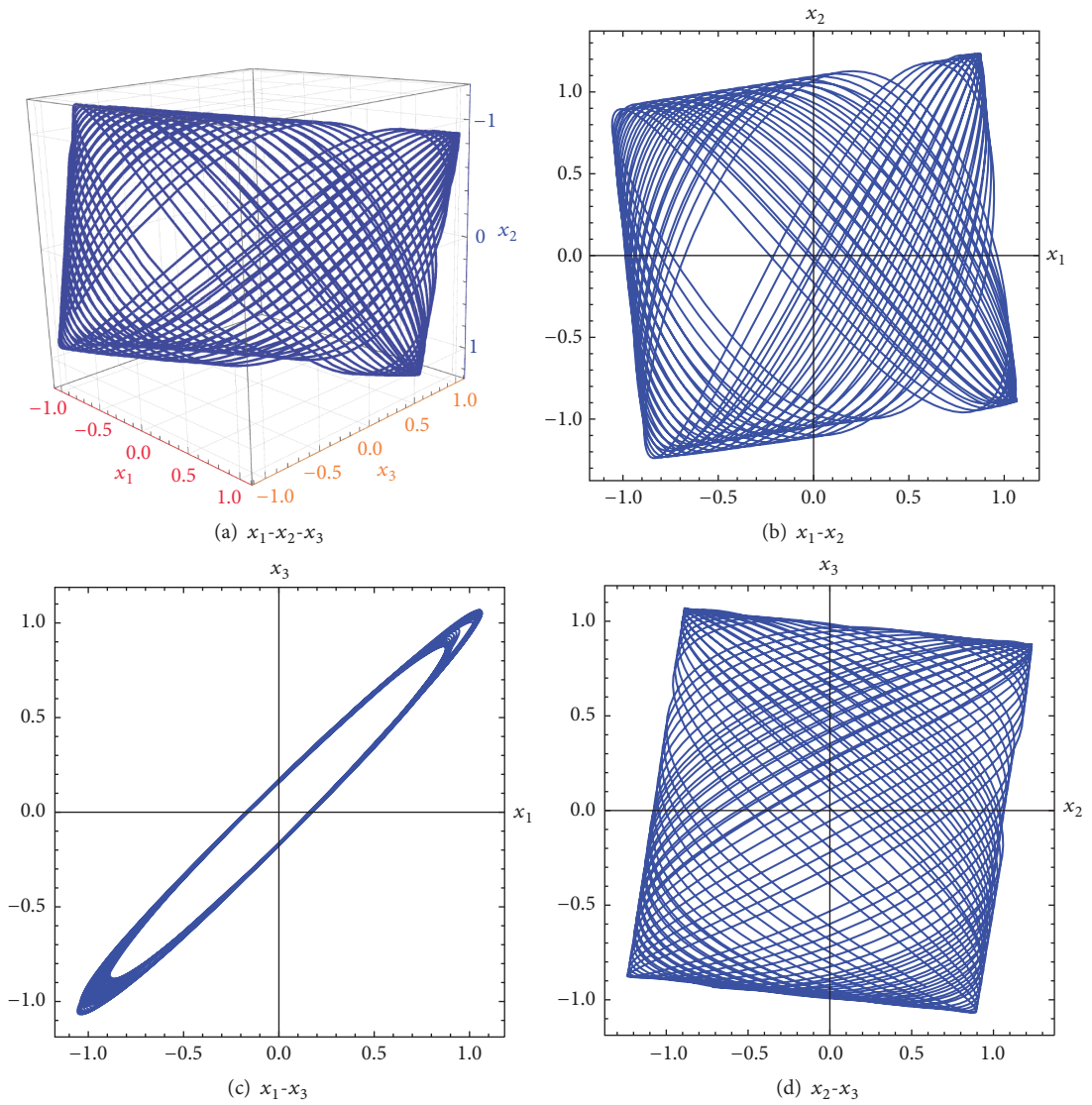

Figure 11: A stable 2D torus of case 2 of ring model obtained when $\varepsilon = 0.1$, $a_1 = 0.45$, $a_2 = 0.3$, $a_3 = -0.2$, $\beta_1 = 1$, $\beta_2 = 2$, $\beta_3 = 1$, and $b_1 = b_2 = b_3 = \alpha_1 = \alpha_2 = \alpha_3 = \alpha_4 = 1$ in system (19).

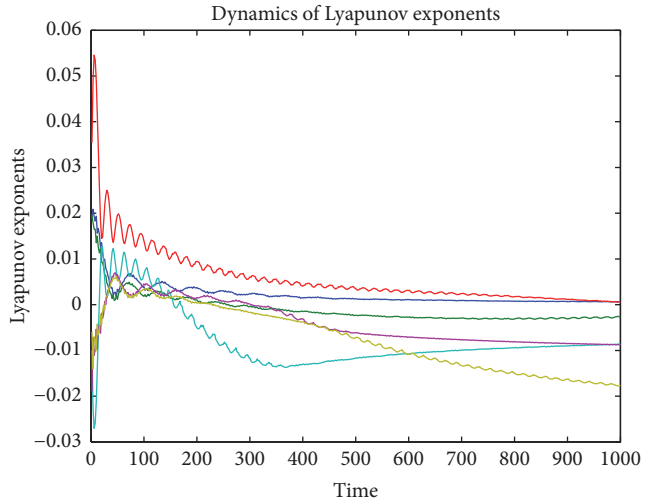

Figure 12: Lyapunov exponents of the equilibrium solution in Figure 11.

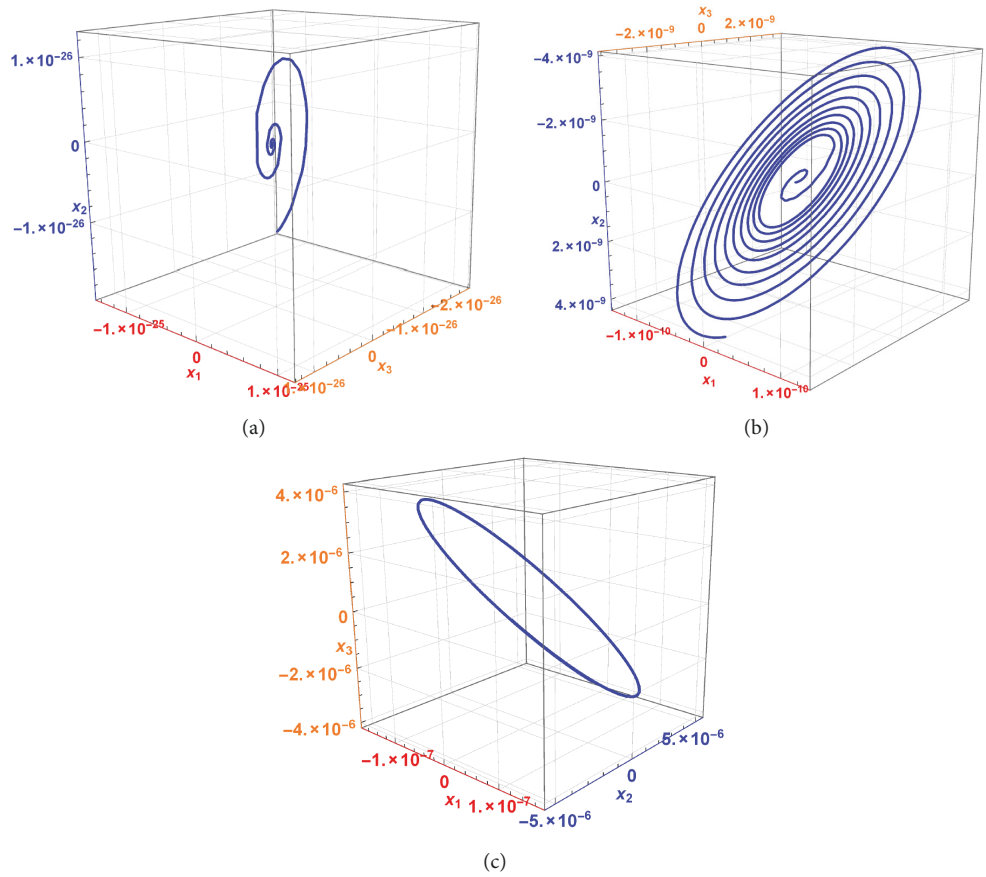

FIGURE 13: Phase portraits of case 1 of ring model with time-delayed coupling obtained for three values of τ, $\varepsilon = 0.1$, $a_1 = -1$, $a_2 = -0.5$, $a_3 = -1$, $\beta_1 = 1$, $\beta_2 = 2$, $\beta_3 = 2$, and $b_1 = b_2 = b_3 = \alpha_1 = \alpha_2 = \alpha_3 = 1$ in system (65). Time delay values are for (a) $\tau = 0.3$, (b) $\tau = 0.4$, and (c) $\tau = 0.6$.

5.1. Numerical Simulation of Case 1 of Ring Model. Some numerical examples of system (18) are given to address the following scenarios. First, when parameters a_1, a_2, and a_3 have negative values, it is found that a stable equilibrium point at the origin exists as shown in Figure 3. This scenario always occurs for values of parameters satisfying conditions (36). Second, a stable periodic orbit appears in system dynamics when parameters a_1 and a_2 have negative values while a_3 is positive. The equilibrium point at the origin loses its stability and this scenario arises for values of parameters satisfying conditions in (39). Periodic orbits are still observed when parameters a_1, a_2, and a_3 satisfy conditions given in (42) and (45). Figure 4 shows the stable periodic orbit that emerges at $a_1 = -0.4$, $a_2 = -0.5$, and $a_3 = 0.7$. In third scenario, parameters a_1 and a_2 are positive while a_3 is negative. In this case, a 2D torus appears as shown in Figure 5. This agrees with previously obtained stability conditions in parameter space given by (47). The Lyapunov exponents spectrum plot associated with the 2D torus case is shown in Figure 6. Note that 2D tori can also be spotted in system dynamics when conditions (49) and (51) are satisfied. Finally, the parameters a_1, a_2, and a_3 are taken positive in numerical simulations. In particular, Figure 7 clarifies the occurrence of 3D torus in phase space of the system at $a_1 = 0.4$, $a_2 = 0.4$, and $a_3 = 0.5$. This case is corresponding to the conditions given in (53). The associated Lyapunov exponents spectrum is plotted and shown in Figure 8.

5.2. Numerical Simulation of Case 2 of Ring Model. The numerical examples of system (19) are shown in Figures 9–12 to illustrate the following scenarios. First, a stable equilibrium point at origin occurs when parameters a_1, a_2, and a_3 are all negative as shown in Figure 9. Setting the values of parameters to satisfy conditions (56) leads to this scenario. Second, when parameters a_1 and a_3 are negative while a_2 is positive, a stable periodic orbit is obtained. The stable equilibrium point at origin becomes unstable and this scenario arises for the values of parameters conditions in (59). A stable periodic orbit is shown in Figure 10 when $a_1 = -0.7$, $a_2 = 0.4$, and $a_3 = -0.5$. Periodic orbits also occur when parameters a_1, a_2, and a_3 satisfy conditions in (62). Finally, a 2D torus appears in system dynamics when parameters a_1 and a_2 are positive while a_3 is negative. This is clarified in Figure 11 where $a_1 = 0.45$, $a_2 = 0.3$, and $a_3 = -0.2$. The values of parameters a_1, a_2, and a_3 in this example satisfy the conditions in (64). The associated Lyapunov exponents spectrum is plotted and shown in Figure 12.

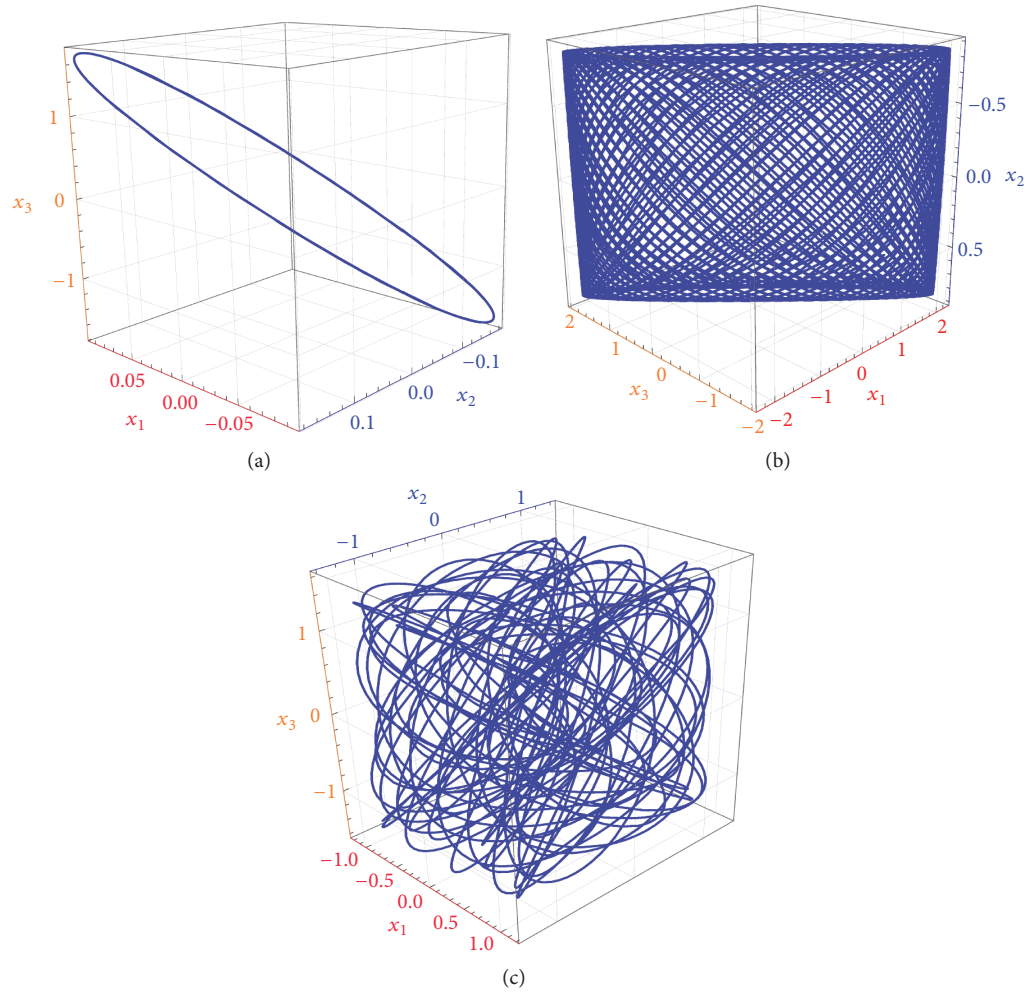

FIGURE 14: Phase portraits of case 1 of ring model with time-delayed coupling obtained for (a) $\tau = 2$, $\varepsilon = 0.1$, $a_1 = -0.4$, $a_2 = -0.5$, $a_3 = 0.7$, $\beta_1 = 1$, $\beta_2 = 2$, $\beta_3 = 3$ and $b_1 = b_2 = b_3 = \alpha_1 = \alpha_2 = \alpha_3 = 1$, (b) $\tau = 2$, $\varepsilon = 0.1$, $a_1 = 0.42$, $a_2 = 0.3$, $a_3 = -0.2$, $\beta_1 = 1$, $\beta_2 = 2$, $\beta_3 = 1$ and $b_1 = b_2 = b_3 = \alpha_1 = \alpha_2 = \alpha_3 = 1$, and (c) $\tau = 1$, $\varepsilon = 0.1$, $a_1 = 0.4$, $a_2 = 0.4$, $a_3 = 0.5$, $\beta_1 = 1$, $\beta_2 = 3$, $\beta_3 = 2$ and $b_1 = b_2 = b_3 = \alpha_1 = \alpha_2 = \alpha_3 = 1$.

5.3. Effects of Time-Delayed Coupling. In this part, the influences of time-delayed coupling on the aforementioned numerical examples are numerically investigated. For case 1 of ring model the mathematical model can be rewritten in the following form:

$$\ddot{x}_j - \varepsilon \dot{x}_j \left(a_j - \alpha_j x_j^2\right) + \beta_j x_j - b_j \varepsilon \left(\sum_{k=1, k\neq j}^{3} x_k^{\tau}\right) = 0, \quad j = 1, 2, 3. \tag{65}$$

$x_k^{\tau} = x_k(t - \tau)$ and τ denotes constant time delay value. It is observed that for the values of parameters used in Figure 13 the equilibrium point loses its stability when time delay value increases over a certain value (approximately 0.4) and a periodic orbit is induced.

However, the effects of time delay coupling on other dynamics of system are almost negligible as shown in Figure 14.

For case 2 of ring model the rate equations can be reformulated as follows:

$$\begin{aligned} &\ddot{x}_1 - \varepsilon \dot{x}_1 \left(a_1 - \alpha_1 x_1^2\right) + \beta_1 x_1 - b_1 \varepsilon \left(x_2^{\tau} + x_3^{\tau}\right) = 0, \\ &\ddot{x}_2 - \varepsilon \dot{x}_2 \left(a_2 - \alpha_3 x_2^3 - \alpha_2 x_2^2\right) + \beta_2 x_2 - b_2 \varepsilon \left(x_1^{\tau} + x_3^{\tau}\right) \\ &\quad = 0, \\ &\ddot{x}_3 - \varepsilon \dot{x}_3 \left(a_3 - \alpha_4 x_3^3\right) + \beta_3 x_3 - b_3 \varepsilon \left(x_1^{\tau} + x_2^{\tau}\right) = 0. \end{aligned} \tag{66}$$

Although the effect of time-delayed coupling on the stable equilibrium point at the origin and torus is measly as shown in Figure 15, it is observed that it has an obvious impact on periodic solution that exists when conditions are satisfied as shown in Figure 16.

6. Conclusion

In this work, we have investigated new analytical results concerning the dynamical behaviors of three coupled memristor-based oscillators with identical and different nonlinearities

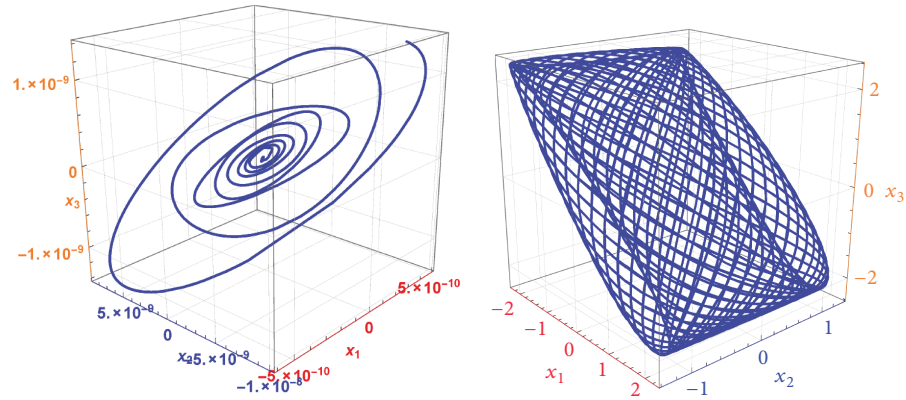

(a) (b)

FIGURE 15: Phase portraits of case 2 of ring model with time-delayed coupling obtained for (a) $\tau = 2$, $\varepsilon = 0.1$, $a_1 = -1$, $a_2 = -1$, $a_3 = -1$, $\beta_1 = 3$, $\beta_2 = 1$, $\beta_3 = 2$ and $b_1 = b_2 = b_3 = \alpha_1 = \alpha_2 = \alpha_3 = \alpha_4 = 1$ and (b) $\tau = 0.5$, $\varepsilon = 0.1$, $a_1 = 0.45$, $a_2 = 0.3$, $a_3 = -0.2$, $\beta_1 = 1$, $\beta_2 = 2$, $\beta_3 = 1$ and $b_1 = b_2 = b_3 = \alpha_1 = \alpha_2 = \alpha_3 = \alpha_4 = 1$.

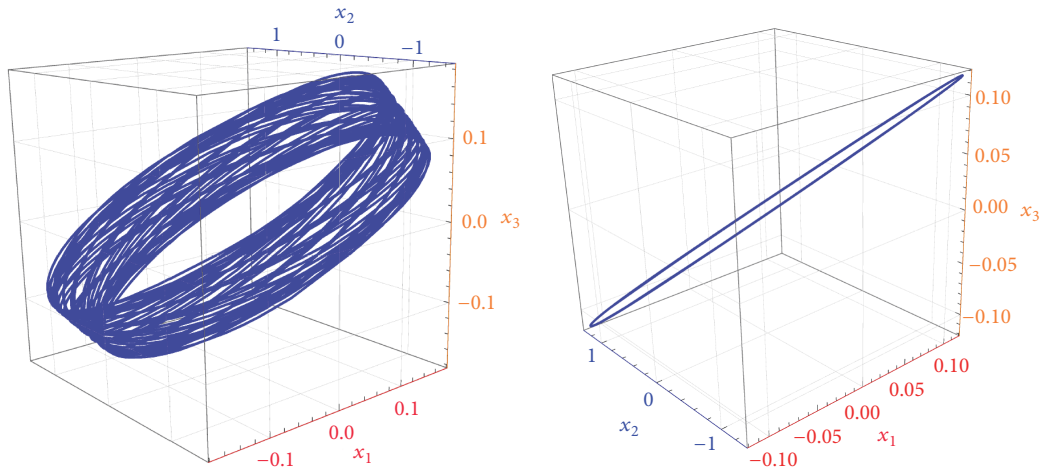

(a) (b)

FIGURE 16: Phase portraits of case 2 of ring model with time-delayed coupling obtained for two values of τ, $\varepsilon = 0.1$, $a_1 = -1$, $a_2 = -0.5$, $a_3 = -1$, $\beta_1 = 1$, $\beta_2 = 2$, $\beta_3 = 2$ and $b_1 = b_2 = b_3 = \alpha_1 = \alpha_2 = \alpha_3 = 1$ in system (66). Time delay values are for (a) $\tau = 0.7$ and (b) $\tau = 0.1$.

in ring configuration. The stability regions in parameters space are attained for each type of induced dynamics. The analytical perturbation techniques were employed to achieve this goal analytically. Furthermore, numerical simulations are performed and they agreed with analytical results obtained. It was demonstrated that the proposed models exhibit complex dynamics including periodic orbits, 2D tori, and 3D tori in ring coupling configuration. A detailed analytical investigations of the effects of time-delayed couplings, with different time delays, can be considered in future work. Also, the mathematical modeling of coupled memristor-based oscillators using fractional order derivatives, in order to accurately incorporate memory effects, can be examined.

Data Availability

The data used to support the findings of this study are included within the article.

Conflicts of Interest

The authors declare that they have no conflicts of interest.

References

[1] S. H. Strogatz, *Nonlinear dynamics and chaos: with applications to physics, biology, chemistry, and engineering*, Hachette, UK, 2014.

[2] R. E. Mirollo and S. H. Strogatz, "Synchronization of pulse-coupled biological oscillators," *SIAM Journal on Applied Mathematics*, vol. 50, no. 6, pp. 1645–1662, 1990.

[3] P. Ashwin, S. Coombes, and R. Nicks, "Mathematical frameworks for oscillatory network dynamics in neuroscience," *Journal of Mathematical Neuroscience*, vol. 6, no. 1, 2016.

[4] S.. Farmer, "Neural rhythms in parkinson's disease, 2002".

[5] C. M. Gray, "Synchronous oscillations in neuronal systems: mechanisms and functions," *Journal of Computational Neuroscience*, vol. 1, no. 1-2, pp. 11–38, 1994.

[6] Ekkehard Ullner and Antonio Politi, "Self-sustained irregular activity in an ensemble of neural oscillators," *Physical Review X*, vol. 6, no. 1, 2016.

[7] M. R. Tinsley, S. Nkomo, and K. Showalter, "Chimera and phase-cluster states in populations of coupled chemical oscillators," *Nature Physics*, vol. 8, no. 9, pp. 662–665, 2012.

[8] A. F. Taylor, M. R. Tinsley, F. Wang, Z. Huang, and K. Showalter, "Dynamical quorum sensing and synchronization in large populations of chemical oscillators," *Science*, vol. 323, no. 5914, pp. 614–617, 2009.

[9] J. A. Acebrón, L. L. Bonilla, C. J. Perez-Vicente, F. Ritort, and R. Spigler, "The Kuramoto model: a simple paradigm for synchronization phenomena," *Reviews of Modern Physics*, vol. 77, no. 1, pp. 137–185, 2005.

[10] S. H. Strogatz, "From Kuramoto to Crawford: exploring the onset of synchronization in populations of coupled oscillators," *Physica D: Nonlinear Phenomena*, vol. 143, no. 1-4, pp. 1–20, 2000.

[11] K. Wiesenfeld and J. W. Swift, "Averaged equations for Josephson junction series arrays," *Physical Review E: Statistical, Nonlinear, and Soft Matter Physics*, vol. 51, no. 2, pp. 1020–1025, 1995.

[12] T. Endo and S. Mori, "Mode Analysis of a Multimode Ladder Oscillator," *IEEE Transactions on Circuits and Systems II: Express Briefs*, vol. 23, no. 2, pp. 100–113, 1976.

[13] S. P. Datardina and D. A. Linkens, "Multimode Oscillations in Mutually Coupled van der Pol Type Oscillators with Fifth-Power Nonlinear Characteristics," *IEEE Transactions on Circuits and Systems II: Express Briefs*, vol. 25, no. 5, pp. 308–315, 1978.

[14] M. Kojima, Y. Uwate, and Y. Nishio, "Multimode oscillations in coupled oscillators with high-order nonlinear characteristics," *IEEE Transactions on Circuits and Systems I: Regular Papers*, vol. 61, no. 9, pp. 2653–2662, 2014.

[15] M. Yoneda, Y. Hosokawa, and Y. Nishio, "Stability analysis of multimode oscillations in two coupled oscillators with ninth-power nonlinearities," *NCSP*, pp. 487–490, 2004.

[16] L. O. Chua, "Memristor—the missing circuit element," *IEEE Transactions on Circuit Theory*, vol. 18, no. 5, pp. 507–519, 1971.

[17] D. B. Strukov, G. S. Snider, D. R. Stewart, and R. S. Williams, "The missing memristor found," *Nature*, vol. 453, pp. 80–83, 2008.

[18] Y. N. Joglekar and S. J. Wolf, "The elusive memristor: properties of basic electrical circuits," *European Journal of Physics*, vol. 30, no. 4, pp. 661–675, 2009.

[19] O. Kavehei, A. Iqbal, Y. S. Kim, K. Eshraghian, S. F. Al-Sarawi, and D. Abbott, "The fourth element: characteristics, modelling and electromagnetic theory of the memristor," *Proceedings of the Royal Society A Mathematical, Physical and Engineering Sciences*, vol. 466, no. 2120, pp. 2175–2202, 2010.

[20] F. Corinto, A. Ascoli, and M. Gilli, "Nonlinear dynamics of memristor oscillators," *IEEE Transactions on Circuits and Systems I: Regular Papers*, vol. 58, no. 6, pp. 1323–1336, 2011.

[21] M. Messias, C. Nespoli, and V. A. Botta, "Hopf bifurcation from lines of equilibria without parameters in memristor oscillators," *International Journal of Bifurcation and Chaos*, vol. 20, no. 2, pp. 437–450, 2010.

[22] T. Endo and S. Mori, "Mode Analysis of a Ring of a Large Number of Mutually Coupled van der Pol Oscillators," *IEEE Transactions on Circuits and Systems II: Express Briefs*, vol. 25, no. 1, pp. 7–18, 1978.

[23] S. H. Jo, T. Chang, I. Ebong, B. B. Bhadviya, P. Mazumder, and W. Lu, "Nanoscale memristor device as synapse in neuromorphic systems," *Nano Letters*, vol. 10, no. 4, pp. 1297–1301, 2010.

[24] A. G. Radwan and M. E. Fouda, *On The Mathematical Modeling of Memristor, Memcapacitor, and Meminductor*, vol. 26 of *Studies in Systems, Decision and Control*, Springer, 2015.

[25] X. Wang, C. Li, T. Huang, and S. Duan, "Predicting chaos in memristive oscillator via harmonic balance method," *Chaos: An Interdisciplinary Journal of Nonlinear Science*, vol. 22, no. 4, 043119, 7 pages, 2012.

[26] T. Driscoll, J. Quinn, S. Klein et al., "Memristive adaptive filters," *Applied Physics Letters*, vol. 97, no. 9, Article ID 093502, 2010.

[27] C. K. Volos, I. M. Kyprianidis, I. N. Stouboulos, E. Tlelo-Cuautle, and S. Vaidyanathan, "Memristor: A new concept in synchronization of coupled neuromorphic circuits," *Journal of Engineering Science and Technology Review*, vol. 8, no. 2, pp. 157–173, 2015.

[28] A. Mittal and S. Swaminathan, "Image stabilization using memristors," in *Proceedings of the 2010 International Conference on Mechanical and Electrical Technology, ICMET 2010*, pp. 789–792, Singapore, September 2010.

[29] B. Muthuswamy and P. Kokate, "Memristor-based chaotic circuits," *IETE Technical Review*, vol. 26, no. 6, pp. 415–426, 2009.

[30] P. K. Roy and A. Basuray, "A high frequency chaotic signal generator: A demonstration experiment," *American Journal of Physics*, vol. 71, no. 1, pp. 34–37, 2003.

[31] A. M. El-Sayed, A. Elsaid, H. M. Nour, and A. Elsonbaty, "Dynamical behavior, chaos control and synchronization of a memristor-based ADVP circuit," *Communications in Nonlinear Science and Numerical Simulation*, vol. 18, no. 1, pp. 148–170, 2013.

[32] Y. Wang and X. Liao, "Stability analysis of multimode oscillations in three coupled memristor-based circuits," *AEÜ - International Journal of Electronics and Communications*, vol. 70, no. 12, pp. 1569–1579, 2016.

[33] X. Wang, X. Liu, K. She, and S. Zhong, "Pinning impulsive synchronization of complex dynamical networks with various time-varying delay sizes," *Nonlinear Analysis: Hybrid Systems*, vol. 26, pp. 307–318, 2017.

[34] X. Wang, X. Liu, K. She, and S. Zhong, "Finite-time lag synchronization of master-slave complex dynamical networks with unknown signal propagation delays," *Journal of The Franklin Institute*, vol. 354, no. 12, pp. 4913–4929, 2017.

[35] X. Wang, X. Liu, K. She, S. Zhong, and L. Shi, "Delay-Dependent Impulsive Distributed Synchronization of Stochastic Complex Dynamical Networks With Time-Varying Delays," *IEEE Transactions on Systems, Man, and Cybernetics: Systems*, pp. 1–9.

[36] A. H. Nayfeh, *The Method of Normal Forms*, Wiley Series in Nonlinear Science, John Wiley & Sons, NY, USA, 1993.